Study of friction and wear behaviors of Fe-based amorphous coatings by MD simulations

Zhenhua Chu[1], Yuyun Zhou[1], Fa Xu[1], Jingxiang Xu[1], Xingwei Zheng[2], Xiaotao Luo[3]*, Yan Shu[4], Zheng Zhang[1] and Qingsong Hu[1]

[1]Department of Mechanical Engineering, College of Engineering, Shanghai Ocean University, Shanghai, China, [2]College of Science, Donghua University, Shanghai, China, [3]State Key Laboratory for Mechanical Behavior of Materials, Xi'an Jiaotong University, Xi'an, China, [4]Ocean Science and Engineering College, Shanghai Maritime University, Shanghai, China

In this study, molecular dynamics simulation is adopted to investigate the friction and wear mechanism of Fe-based amorphous composited coatings. It was found that the ceramic phase can improve plasticity of the composite coatings to reduce wear. In addition, when the Al_2O_3 content is 15 wt%, due to the stress concentration between ceramic phase and amorphous phase, the viscosity flow in the amorphous phase results in plastic deformation. Through this, the best wear resistance has been obtained. In addition, with the increase of compression depth, the number of atoms accumulated constantly increases, and the degree of plastic deformation becomes higher in the composite coatings. Finally, a high sliding speed results in the reduction of the wear resistance of coatings.

Introduction

In addition to high corrosion resistance, it is required that the structural materials of offshore equipment have high wear resistance due to sediment erosion in the marine environment. Bulk metallic glass, known as amorphous alloy, is a new material with high strength, and superior corrosion and wear resistance, and has attracted the attention of many researchers (Chiang et al., 2010; Lee et al., 2010; Chu et al., 2012). It can be used as a coating by a spraying method. Meanwhile, the wear resistance of the coating has been studied widely. Zhang and Liu et al. (Zhang et al., 2012) studied the wear behavior of high velocity oxygen fuel (HVOF)-sprayed Fe-based amorphous coatings. However, due to the structural characteristics of amorphous alloy, there is no dislocation and phase boundary, leading to plastic deformation and poor toughness. This leads to cracks developing quickly and crossing the coating surface. Especially for coatings used in marine conditions, local peeling of the coating accelerates its failure.

In order to improve the toughness of Fe-based amorphous coatings, composite coatings were fabricated. Yasir et al. (Yasir et al., 2015) found that composite coatings exhibited improved wear resistance and reduced the coefficient of friction (COF) in both air and wet conditions as compared to the monolithic amorphous coating. Chu (Chu et al., 2019a) studied the wear resistance of Fe-based composite coatings with Al_2O_3 and found the best wear resistance with 15 wt% Al_2O_3. Many experimental studies have been performed on the wear behaviors of Fe-based amorphous coatings. However, the essence of friction and wear is a dynamic progression of atom movement, and because the structure of amorphous alloys is different to metallic alloys, the deformation mechanism needs to be well investigated.

It is rather difficult to directly observe the progression of friction on materials by *in situ* experiments with atomic-scale resolution, but molecular dynamics (MD) allows the wear mechanism at a nanoscale level to be revealed. Han et al. (Han et al., 2019) performed MD simulations to investigate the friction and wear behaviors of $Ti_2AlN/TiAl$ composite. Sun et al. (Sun et al., 2017) investigated the tire-aggregate friction mechanism by MD simulation. Kim and Chung (Kim and Chung, 2020) conducted molecular dynamics simulations to investigate the contact condition between nominally flat surfaces. Ji et al. (Ji et al., 2019) investigated the roles of nanoparticles in the sliding friction process at a nanoscale level using molecular dynamics simulations. Due to the structural characteristics of amorphous materials with ordered short-range and disordered long-range atomic order, the deformation mechanism is different to metallic alloys. MD simulation is beneficial to understand the deformation mechanism during the sliding process (Meacci et al., 2019; Sun and Wing, 2019; Hua et al., 2020; Nguyen, 2021; Luo et al., 2022), particularly regarding the effect of additions into the amorphous matrix on the wear mechanism.

In this study, we perform MD simulation to investigate the friction and wear behaviors of Fe-based amorphous coatings. In addition, the effects of Al_2O_3 content, compression depth, and sliding speed on material are thoroughly investigated. In addition, a deformation mechanism is proposed by the results of MD simulation.

Experiment process

MD simulation model

$Fe_{54}Cr_{25}Mo_{17}C_2B_2$ alloy amorphous powders were produced by high pressure atomized Ar gas. In order to evaluate the wear behavior of different levels of Al_2O_3, we construct five models: pure Fe-based amorphous model; 5 wt% Al_2O_3/Fe amorphous composite model; 10 wt% Al_2O_3/Fe amorphous composite model; 15 wt% Al_2O_3/Fe amorphous composite model; and 20 wt% Al_2O_3/Fe amorphous composite model.
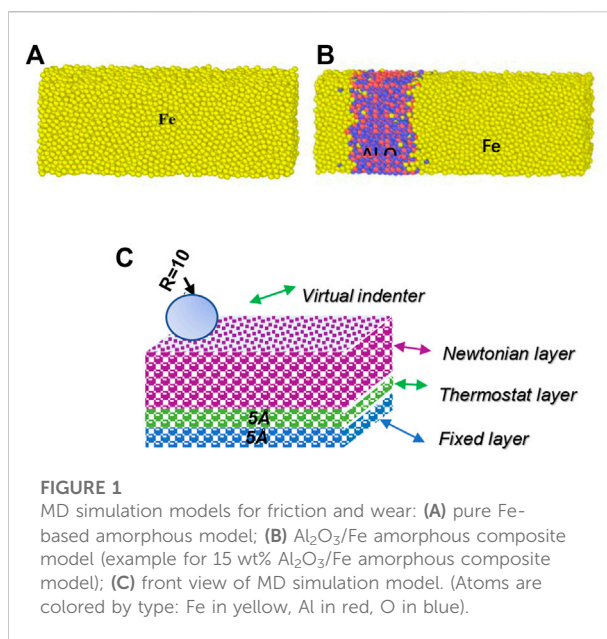

FIGURE 1
MD simulation models for friction and wear: **(A)** pure Fe-based amorphous model; **(B)** Al_2O_3/Fe amorphous composite model (example for 15 wt% Al_2O_3/Fe amorphous composite model); **(C)** front view of MD simulation model. (Atoms are colored by type: Fe in yellow, Al in red, O in blue).

TABLE 1 Parameters of MD simulation.

Box dimension	230(Å)*41.613(Å)*39.349(Å)
Total number of atoms	(a) 12,500; (b) 17,900
Timestep	0.001 ps
Spherical diamond indenter radius	10Å
Depression depth	5Å, 7Å, 9Å
Friction velocity	1 Å/ps, 1.7 Å/ps, 7 Å/ps

As shown in Figures 1A,B pure Fe-based amorphous coating model and an amorphous composite coating model (example of 15 wt% Al_2O_3/Fe amorphous composite amorphous model) are constructed in this study. In the simulation process, the size of the MD system is 230Å*41.613Å*39.349Å. The models are mainly composed of a diamond grinding ball and amorphous coating substrate. The upper part of the model is the indenter, which is a sphere with a radius of 10Å. The center of the sphere is located at x = -25Å, y = 20.8015Å, and z = 54.349Å. Detailed parameters of the MD simulation are shown in Table 1. The substrate is composed of three kinds of atoms: fixed atoms, thermostat atoms, and Newtonian atoms (Liu et al., 2007; Si et al., 2012). As depicted in Figure 1C, the free boundary condition is applied in the *z* direction and the periodic boundary in the *x* and *y* directions. The atoms at the bottom of the substrate with a thickness of 5Å are fixed atoms, which prevent the simulation models from shifting. Thermostat atoms with a thickness of 5Å are adjacent to the fixed atoms in order to dissipate heat. The remainder are Newtonian atoms.
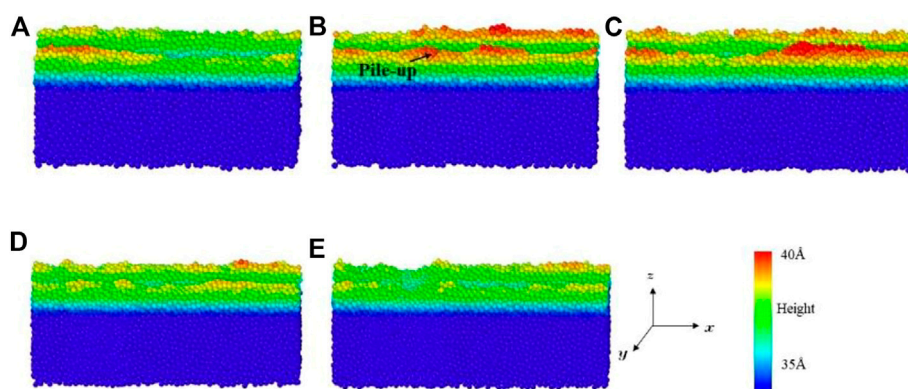
FIGURE 2
Scratched surfaces in the five different Al_2O_3 content models at 400 ps: **(A)** pure Fe-based amorphous model; **(B)** 5 wt% Al_2O_3/Fe amorphous composite model; **(C)** 10 wt% Al_2O_3/Fe amorphous composite model; **(D)** 15 wt% Al_2O_3/Fe amorphous composite model; **(E)** 20 wt% Al_2O_3/Fe amorphous composite model.

Simulation steps

The MD simulation with large-scale atomic/molecular massively parallel simulator (LAMMPS) is adopted to simulate the atomic-scale friction behaviors of contact between a diamond surface and an amorphous surface. There are six different atomic interactions in the simulation, concerning Fe-Fe, Fe-Al, Al-Al, Fe-O, Al-O, and O-O atoms in the substance. In this study, we adopt embedded atom potential (EAM), Morse potential, and Comb3 potential to describe the interaction of the atoms. After constructing the models, a periodic boundary is applied in three directions. In order to stabilize the energy, we adopt combined gradient (CG) to minimize the system temperature constant (300 K).

MD was performed using microcanonical ensemble (also known as NVT ensemble) for a time period of 80 ps with a timestep of 1 fs.

After relaxation progresses, indentation begins, and the intender slides along the surface of the substrate. The simulation process includes indentation and scratching. In the indentation stage, the indenter is placed on the top of 5Å of the substance. Within the NVE ensemble, the indenter above the left side moves downward with a speed of 1.0 Å/ps until the depression depth reaches 7Å. In the scratching stage, the intender moves along the positive side of the x-axis with a speed of 1.0 Å/ps. After the whole models reaches a balanced state, the sliding process starts. The total sliding time of friction is 400 ps. After the MD simulation, the atomic information is visualized by the Open Visualization Tool (OVITO).

Sliding experimental process

A ball-on-disc friction-wear tester (SFT-2M, Zhongkekaihua, Technology development Co., Ltd., China) is adopted to evaluate the tribological properties of Fe-based metallic glassy coating and the sliding of composite coatings against commercially obtained Si_3N_4 balls (5 mm in diameter) in air. Each test was carried out using an applied load of 30 N. The sliding speed was selected at a constant value of 500 r/min, and the duration of sliding was 15 min.

Results and discussions

Wear behaviors of different Al_2O_3 content simulation models

In order to investigate the wear process, wear morphologies were studied. Figure 2 shows the scratched surfaces of the five simulation models at 400 ps. Usually, the wear proportion can be evaluated by the number of worn atoms in the pile-up. Compared to Figure 2A, the pile-up significantly increases in Figure 2B. It can be observed that the worn atomic number gradually increases and then decreases.

In order to further explain the abrasive resistance of the five simulation models, a cross-section is selected at a time of 400 ps. As shown in Figure 3, the compression depth of the models firstly increases and then gradually decreases. In addition, the data in the diagram are based on the change in the location of different atoms (shown in Figure 4). From this, we can confirm that the compression depth is the lowest when the Al_2O_3 content is 15 wt%. Above all, the effect of friction coefficient, wear rate and compression depth, and the abrasive resistance of the 15 wt% Al_2O_3 composite model are at optimum levels. This is consistent with results from the previous experiment.

Experimental wear behaviors of different Al_2O_3 content

In order to verify the reliability of the simulation data, they were compared to experimental data. The sliding wear
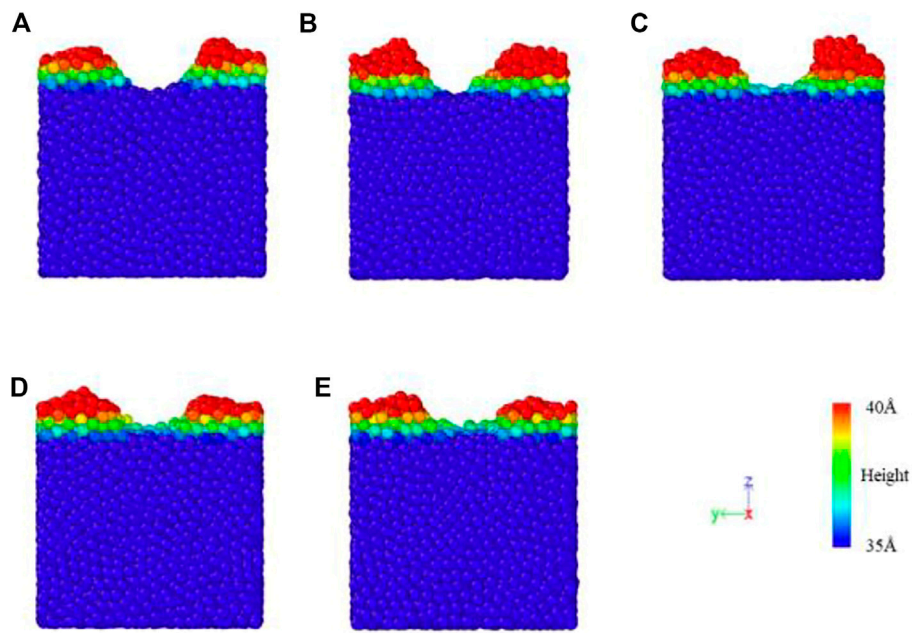
FIGURE 3
The scratch depth of different Al_2O_3 content in 400 ps: **(A)** pure Fe-based amorphous model; **(B)** 5 wt% Al_2O_3/Fe amorphous composite model; **(C)** 10 wt% Al_2O_3/Fe amorphous composite model; **(D)** 10 wt% Al_2O_3/Fe amorphous composite model; **(E)** 20 wt% Al_2O_3/Fe amorphous composite model.
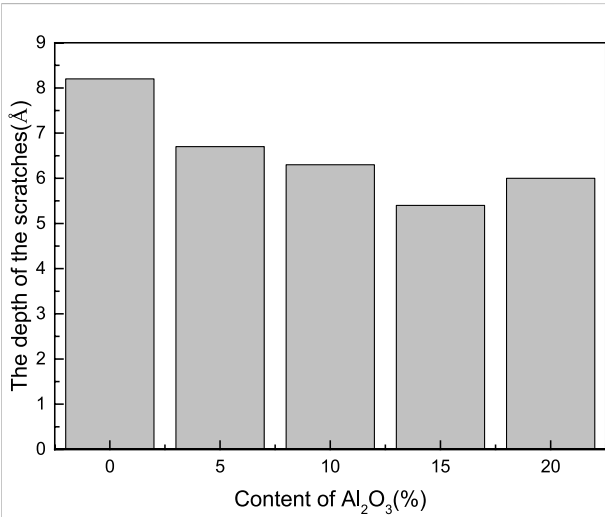

FIGURE 4
The curve of content of Al_2O_3 and the depth of the scratches.
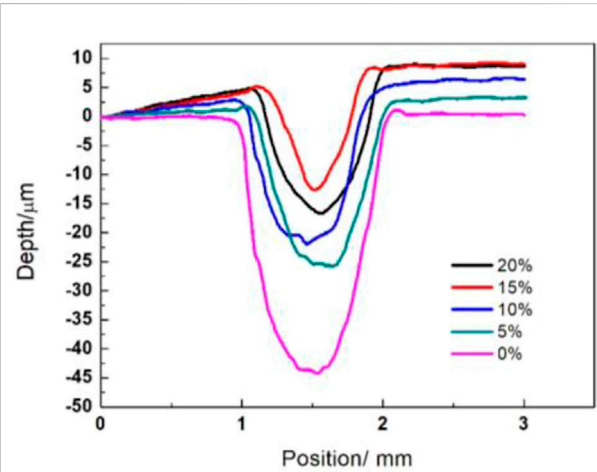

FIGURE 5
Measurement of wear profile of AT13/Fe-based amorphous composite coatings (0−20 wt.%Al_2O_3).

performance of the coatings can be characterized by measuring the surface profile of the coating wear scar. Figure 5 shows the wear depth of the coatings with various Al_2O_3 content. The wear depth of the Fe-based amorphous coating is the largest, reaching 44 μm, which indicates that the coating has incurred serious wear during the grinding process with the Si_3N_4 friction pair. With an increase of Al_2O_3 content in the second phase of the composite coating, the wear depth decreases gradually, and when Al_2O_3 content increases to 15 wt%, the wear depth is the lowest. When
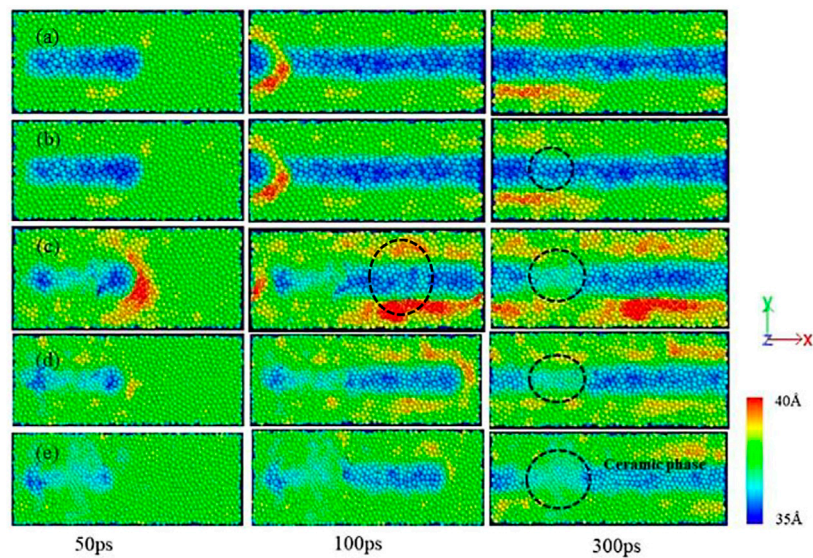
FIGURE 6
Atomistic representations of different Al$_2$O$_3$ content models: **(A)** pure Fe-based amorphous model; **(B)** 5 wt% Al$_2$O$_3$/Fe amorphous composite model; **(C)** 10 wt% Al$_2$O$_3$/Fe amorphous composite model; **(D)** 10 wt% Al$_2$O$_3$/Fe amorphous composite model; **(E)** 20 wt% Al$_2$O$_3$/Fe amorphous composite model.

Al$_2$O$_3$ content is further increased to 20 wt% in the second phase, the wear depth no longer decreases, but it is still higher than that of the Fe-based amorphous coating. This conclusion is consistent with the results of simulation.

Wear mechanism of the coatings with different Al$_2$O$_3$ content

Since it is rather difficult to directly observe progression of friction on materials by *in situ* experiments with atomic-scale resolution, MD simulation can show the motion of atoms during the sliding process. It is beneficial to understand the wear mechanism, especially for metallic glassy composite materials. Figure 6 shows the surface morphology evolution of five models with different Al$_2$O$_3$ content at 50 ps, 100 ps, and 300 ps during the sliding process. The atoms are colored according to height. A groove can be seen that has formed in the surface, and both sides of the groove have obvious material accumulation. Meanwhile, with the sliding process, the wear depth of both Fe-based amorphous coatings and composite coatings increased. However, compared with the composite coating, the wear depth of Fe-based amorphous coating is deeper, and the wear scar width is larger. At a time of 50 ps in the early stage of wear, the visible surface height clearly increases at the interface between the Al$_2$O$_3$ ceramic phase and the amorphous phase (as circled in Figure 6 (c) at 50 ps). This is due to the different elastic modulus of the Al$_2$O$_3$ ceramic phase and amorphous phase. The deformation degree of the two phases is

different at load, resulting in stress concentration at the interface. The high stress induces the development of shear bands in the amorphous phase, which promotes the large plastic deformation of the amorphous coating (Chu et al., 2019b). In composite coatings, a plastic deformation zone around the indentation is observed. With regards to the wear resistance of the material, besides high levels of strength and hardness, a good plastic deformation ability is also an important factor affecting wear resistance. In other words, a material that maintains high strength while also having good plasticity will achieve the purpose of resisting crack propagation. In Figure 6 (c) and (d), plastic deformation zones are observed in the 10% and 15% Al$_2$O$_3$ composite coatings. Although Al$_2$O$_3$ was added during the brittle phase, the material stills shows fatigue wear due to the sliding process. The high stress concentration between the amorphous phase and ceramic phase results in viscosity flow in the amorphous phase, and the increase in height can be observed in the composite coatings. However, when the addition of Al$_2$O$_3$ is more than 20%, the fatigue wear of the ceramic phase increases.

The impact of compression depth on the friction and wear behaviors of Fe-based amorphous and 15 wt% composite models

In this study, three compression depths of 5Å, 7Å, and 9Å are chosen in order to explain the effect of compression depth on the friction and wear behavior of Fe-based metallic glassy coating and 15 wt % composite models. In MD simulation, the friction speed is 1.0 Å/ps.
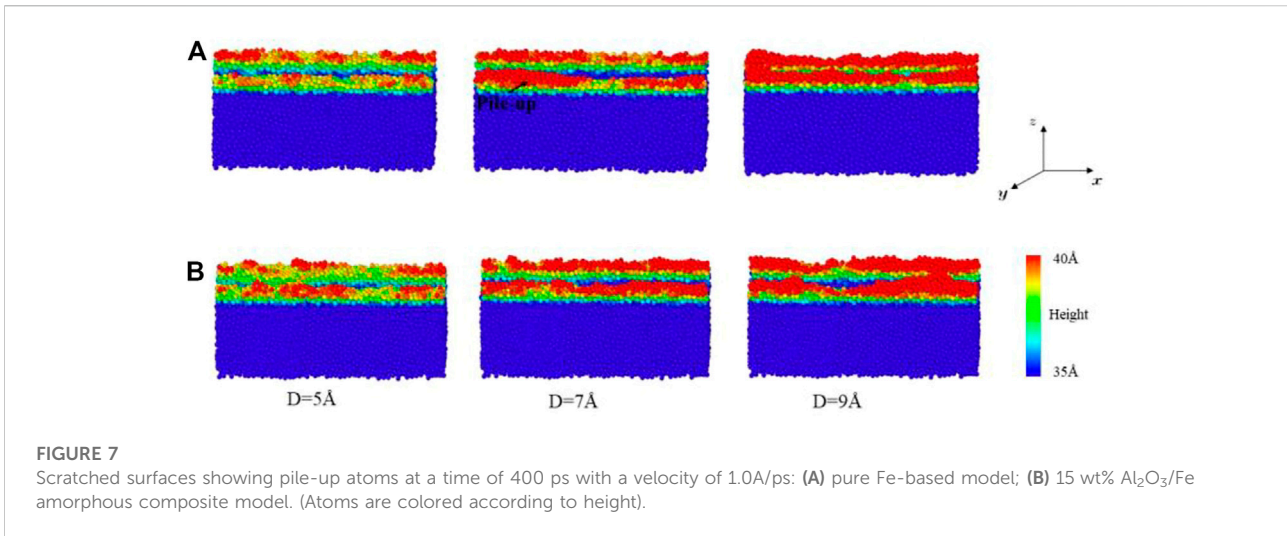
FIGURE 7
Scratched surfaces showing pile-up atoms at a time of 400 ps with a velocity of 1.0A/ps: **(A)** pure Fe-based model; **(B)** 15 wt% Al_2O_3/Fe amorphous composite model. (Atoms are colored according to height).
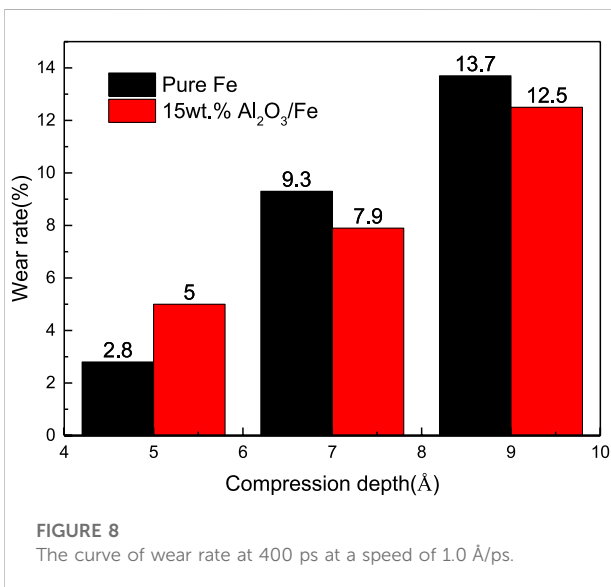

FIGURE 8
The curve of wear rate at 400 ps at a speed of 1.0 Å/ps.

Figure 7 shows scratched surfaces showing pile-up atoms at the time of 400 ps with a speed of 1.0 Å/ps. It is clear that the wear degree of the substance surface gradually increases as the compression depth increases. This is because the number of atoms that push on both sides and from above increase relatively with an increase in compression depth. In other words, the friction volume accumulated in front of the indenter is relatively larger, which leads to a compression depth proportional to the wear rate. At the same time, the wear degree of the 15 wt% Al_2O_3 composite model is proportionally lower than that of the Fe-based metallic glassy coating model. This indicates that the abrasive

resistance of the amorphous composite coating is higher than the Fe-based amorphous coating. As shown in Figure 8, the wear rate gradually increases with an increase of compression depth. It is worth noting that the wear rate of the composite coating is higher than the Fe-based amorphous coating at a compression depth of 5Å. Following an increase of compression depth, the wear rate of the composite coating is lower than pure Fe-based amorphous coating. This is because with an increased compression depth, the distance between the atoms that are situated between the indenter and the substances decreases, resulting in the increased resistance of the atoms. The compressed atoms on the surface of the material display compressional deformation. During friction, the number of atoms accumulated continually increases, and the level of plastic deformation becomes deeper. Above all, an increase in compression depth is positive for the wear of materials, and the wear resistance of composite coating is superior to Fe-based amorphous coating.

The impact of sliding speed on the friction and wear behaviors of Fe-based amorphous and 15 wt% composite models

According to the classification of sliding speeds for friction (Fang et al., 2014; Li et al., 2014), a general frictional speed is less than 0.45 Å/ps, a high frictional speed is 0.45–1.5 Å/ps, and an ultra-high frictional speed is more than 1.5 Å/ps. To further analyze the effects of sliding speed on materials, we chose five speeds: 0.1 Å/ps, 0.4 Å/ps, 1.0 Å/ps, 1.7 Å/ps, and 2.7 Å/ps. During MD simulation, the compression depth is maintained at 7Å. Figure 9A shows the evolution of the worn particles of the 15 wt% composite model as a result of different timesteps. It was found that the number
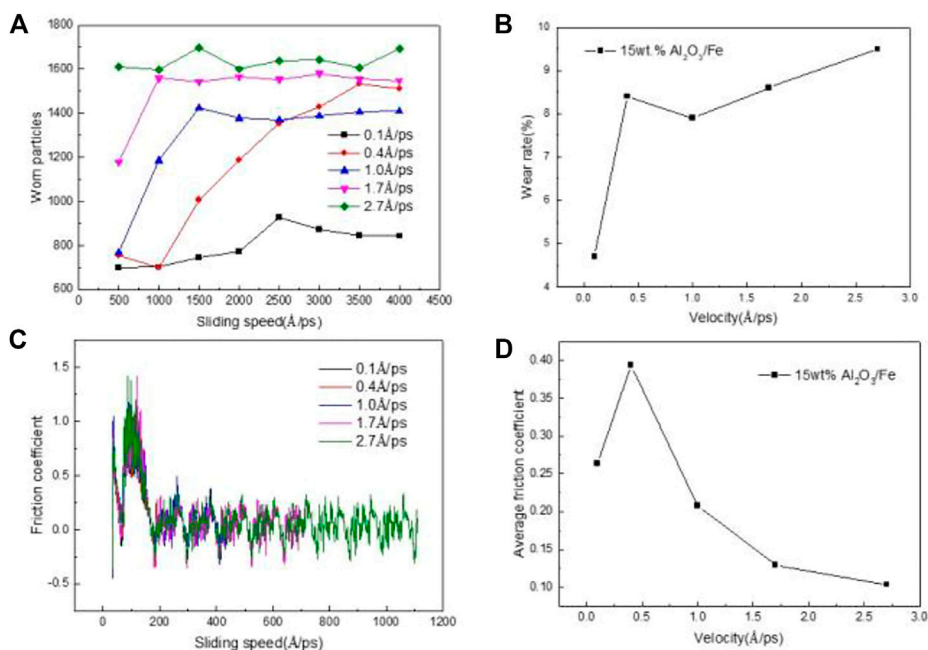
FIGURE 9
(A) Variation of worn particles with sliding distance in 15 wt% Al$_2$O$_3$/Fe amorphous composite model; **(B)** variation of wear rate with different speeds in 15 wt% Al$_2$O$_3$/Fe amorphous composite model; **(C)** variation of friction coefficient with sliding distance in 15 wt% Al$_2$O$_3$/Fe amorphous composite model; **(D)** variation of average friction coefficient with different speeds in 15 wt% Al$_2$O$_3$/Fe amorphous composite model.

of wear particles gradually increases with the timestep. When the time reaches 1,500 ps, the rate of increase of the number of worn particles begins to slows down; the faster the sliding speed, the earlier the time of wear. As illustrated in Figure 9B, sliding speed has a great impact on wear in the initial stage. The wear rate increases with the sliding speed and then maintains a linear growth. In our study, the indenter was set to measure specific parameters, and we have ignored the effects of bond wear on materials. According to the analysis, the relative sliding speed and surface area increase relatively with an increase in sliding speed, eventually leading to an increase in the degree of wear.

Figure 9C shows the changes between sliding distance and friction coefficient at different sliding speeds. The friction coefficient generally decreases as the sliding distance increases. On the other hand, fluctuation of the friction coefficient mainly occurs at the early stage, after which it remains stable. As shown in Figure 9D, the average friction coefficient shows a trend of increasing, and then decreasing and remaining stable. The results show that changes in speed have great impact on the degree of wear of a material under general and high frictional speed. However, at an ultra-high frictional speed, there is no obvious influence on the degree of wear of the material.

Conclusion

In this study, a molecular dynamics simulation is adopted to investigate the friction and wear mechanisms of Fe-based amorphous composited coatings. The MD simulation results are consistent with experimental results, which indicates that the simulation results are reliable. The sliding results show that the Fe-based amorphous composite coating with 15% Al$_2$O$_3$ had best wear resistance. Stress concentration between amorphous phase and ceramic phase results in viscosity flow in the amorphous phase, which improves the plastic deformation, thereby improving wear resistance. Meanwhile, with an increase in compression depth, an increase in the number of atoms accumulated is observed. This means that the level of plastic deformation has become deeper in the composite coatings. It is worth noting that a high sliding speed results in a reduction of the wear resistance of coatings.

Data availability statement

The original contributions presented in the study are included in the article/supplementary material, further inquiries can be directed to the corresponding author.

Author contributions

Funding

Conflict of interest

The authors declare that the research was conducted in the absence of any commercial or financial relationships that could be construed as a potential conflict of interest.

Publisher's note

All claims expressed in this article are solely those of the authors and do not necessarily represent those of their affiliated organizations, or those of the publisher, the editors and the reviewers. Any product that may be evaluated in this article, or claim that may be made by its manufacturer, is not guaranteed or endorsed by the publisher.

References

Chiang, P.-T., Chen, G.-J., Jian, S.-R., Shih, Y.-H., Jang, J. S.-C., and Lai, C.-H., Surface antimicrobial effects of Zr61Al7.5Ni10Cu17.5Si4 thin film metallic glasses on *Escherichia coli*, *Staphylococcus aureus*, *Pseudomonas aeruginosa*, acinetobacter baumannii and Candida albicans, *Fooyin J. Health Sci.* 2 (2010) 12–20. doi:10.1016/S1877-8607(10)60008-2

Chu, J. P., Jang, J. S. C., Huang, J. C., Chou, H. S., Yang, Y., Ye, J. C., et al. (2012). Thin film metallic glasses: Unique properties and potential applications. *Thin Solid Films* 520, 5097–5122. doi:10.1016/j.tsf.2012.03.092

Chu, Z., Wei, F., Zheng, X., Zhang, C., and Yang, Y. (2019). Microstructure and properties of TiN/Fe-based amorphous composite coatings fabricated by reactive plasma spraying. *J. Alloys Compd.* 785, 206–213. doi:10.1016/j.jallcom.2019.01.171

Chu, Z., Zheng, X., Zhang, C., Xu, J., and Gao, L. (2019). Study the effect of AT13 addition on the properties of AT13/Fe-based amorphous composite coatings. *Surf. Coat. Technol.* 379 (379), 125053–125060. doi:10.1016/j.surfcoat.2019.125053

Fang, Q., Liu, Y., and Zhang, L. (2014). A molecular dynamics investigation into the mechanisms of subsurface damage and material removal of monocrystalline copper subjected to nanoscale high speed grinding. *Appl. Surf. Sci.* 303, 331–343. doi:10.1016/j.apsusc.2014.02.178

Han, X., Liu, P., Sun, D., and Wang, Q. (2019). An atomic-level understanding of the friction and wear behaviors of Ti2AlN/TiAl composite via MD simulations. *Tribol. Int.* 137, 340–348. doi:10.1016/j.triboint.2019.05.021

Hua, N., Zhang, X., Liao, Z., Hong, X., Guo, Q., Huang, Y., et al. (2020). Dry wear behavior and mechanism of a Fe-based bulk metallic glass: Description by hertzian contact calculation and finite-element method simulation. *J. Non-Crystalline Solids* 543, 120065. doi:10.1016/j.jnoncrysol.2020.120065

Ji, C., Sun, S., Wang, B., and Lin, B. (2019). Molecular dynamic simulations of the roles of nanoparticles in sliding friction process. *Chem. Phys. Lett.* 728, 44–49. doi:10.1016/j.cplett.2019.04.076

Kim, H.-J., and Chung, K.-H. (2020). Atomistic investigation of the effect of contact condition on frictional properties of nanowire. *Appl. Surf. Sci.* 534, 147629. doi:10.1016/j.apsusc.2020.147629

Lee, C. J., Lin, H. K., Sun, S. Y., and Huang, J. C. (2010). Characteristic difference between ITO/ZrCu and ITO/Ag bi-layer films as transparent electrodes deposited on PET substrate. *Appl. Surf. Sci.* 257, 239–243. doi:10.1016/j.apsusc.2010.06.074

Li, J., Fang, Q., Zhang, L., and Liu, Y. (2014). Subsurface damage mechanism of high speed grinding process in single crystal silicon revealed by atomistic simulations. *Appl. Surf. Sci.* 324, 464–474. doi:10.1016/j.apsusc.2014.10.149

Liu, C., Yu, K., Shi, X., Wang, J., Lam, P. K. S., Wu, R. S. S., et al. (2007). Induction of oxidative stress and apoptosis by PFOS and PFOA in primary cultured hepatocytes of freshwater tilapia (*Oreochromis niloticus*). *Aquat. Toxicol.* 82, 135–143. doi:10.1016/j.aquatox.2007.02.006

Luo, J., Song, J., Moradi, Z., Safa, M., and Khadimallah, M. A. (2022). Effect of simultaneous compressive and inertia loads on the bifurcation stability of shear deformable functionally graded annular fabrications reinforced with graphenes. *Eur. J. Mech. - A/Solids* 94, 104581. doi:10.1016/j.euromechsol.2022.104581

Meacci, M., Shi, Z., Butini, E., Marini, L., Meli, E., and Rindi, A. (2019). A local degraded adhesion model for creep forces evaluation: An approximate approach to the tangential contact problem. *Wear* 203084, 203084–203441. doi:10.1016/j.wear.2019.203084

Nguyen, C. T. (2021). Characteristics of force transmission in cohesive agglomerates impacting a rigid surface. *Mech. Res. Commun.* 117, 103773. doi:10.1016/j.mechrescom.2021.103773

Si, L., Guo, D., Luo, J., and Xie, G. (2012). Planarization process of single crystalline silicon asperity under abrasive rolling effect studied by molecular dynamics simulation. *Appl. Phys. A* 109, 119–126. doi:10.1007/s00339-012-7026-z

Sun, F., Hou, Y., Wang, L., Huang, L., and Qian, Z. (2017). A molecular dynamics (MD) simulation on tire-aggregate friction. *Int. J. Pavement Res. Technol.* 10, 343–351. doi:10.1016/j.ijprt.2017.03.009

Sun, W., and Wing, Y. (2019). Molecular dynamics simulations of friction forces between silica nanospheres. *Comput. Mater. Sci.* 162, 96–110. doi:10.1016/j.commatsci.2019.02.025

Yasir, M., Zhang, C., Wang, W., Xu, P., and Liu, L. (2015). Wear behaviors of Fe-based amorphous composite coatings reinforced by Al2O3 particles in air and in NaCl solution. *Mater. Des.* 88, 207–213. doi:10.1016/j.matdes.2015.08.142

Zhang, C., Liu, L., Chan, K. C., Chen, Q., and Tang, C. Y., Wear behavior of HVOF-sprayed Fe-based amorphous coatings, *Intermetallics* 29 (2012) 80–85. doi:10.1016/j.intermet.2012.05.004